



Adaptive Control Strategy of Active Power Filter for Harmonic Compensation of Non Linear Loads

P SriKavitha¹ B Subba Reddy²

MTECH Scholar, Department of EEE, KIET Kakinada, India.¹

Asso. Professor, Department of EEE, KIET, Kakinada,

Abstract—A dynamic power channel executed with a four-leg voltage-source inverter utilizing a prescient control conspire is exhibited. The utilization of a four-leg voltage-source inverter permits the remuneration of current consonant parts, and in addition lopsided current created by single-stage nonlinear burdens. A point by point yet basic numerical model of the dynamic power channel, including the impact of the proportional power framework impedance, is determined and used to outline the prescient control calculation.

A fluffy controller is intended to relieve the aggregate symphonious contortion. The pay execution of the proposed dynamic power channel and the related control plot under relentless state and transient working conditions is shown through recreations utilizing MATLAB/SIMULINK condition.

File Terms—Active power channel, current control, four-leg converters, prescient control, fluffy controller.

Introduction

Inexhaustible age influences control quality because of its nonlinearity, since sun oriented age plants and wind control generators must be associated with the network through high-control static PWM converters. The nonuniform idea of energy age straightforwardly influences voltage control and makes voltage contortion in control frameworks. This new situation in control appropriation frameworks will require more complex pay systems.

Albeit dynamic power channels executed with three-stage four-leg voltage-source inverters (4L-VSI) have just been exhibited in the specialized writing, the essential commitment of this paper is a prescient control calculation planned and actualized particularly for this application. Customarily, dynamic power channels have been controlled utilizing pretuned controllers, for example, PI-type or versatile, for the present and for the dc-voltage circles. PI controllers must be composed in light of the proportional direct model, while prescient controllers utilize the nonlinear model, which is nearer to genuine working conditions.

A fluffy controller is likewise outlined in the place of PI controller to diminish the sounds. A precise model acquired utilizing prescient controllers enhances the execution of the dynamic power channel, particularly amid transient working conditions, since it can rapidly take after the present reference flag while keeping up a steady dc-voltage. Up until this point, usage of prescient control in control converters have been utilized chiefly in acceptance engine drives. On account of engine drive applications, prescient control speaks to an exceptionally natural control conspire that handles multi variable qualities, rearranges the treatment of dead-time pay, and allows beat width modulator substitution. Notwithstanding, these sorts of utilizations show impediments identified with motions and precariousness made from obscure load parameters. One preferred standpoint of the proposed calculation is that it fits well in dynamic power channel applications, since the power converter yield parameters are outstanding. These yield parameters are acquired from the converter yield swell channel and the power framework proportional impedance. The converter yield swell channel is a piece of the dynamic power channel outline and the power framework impedance is gotten from surely understood standard strategies. On account of obscure framework impedance parameters, an estimation strategy can be utilized to infer an exact R–L proportionate impedance model of the framework.

This paper shows the numerical model of the 4L-VSI and the standards of task of the proposed prescient control conspire, including the plan technique. The total portrayal of the chose current reference generator actualized in the dynamic power channel is likewise exhibited. At long last, the proposed dynamic power channel and the viability of the related control conspire pay are shown through MATLAB/SIMULINK condition.

I. FOUR-LEG CONVERTER MODEL

A dynamic power channel is associated in parallel at the purpose of basic coupling to repay current music, current unbalance, and receptive power. It is created by an electrolytic capacitor, a four-leg PWM converter,

and a first-arrange yield swell channel, as appeared in Fig. 1. This circuit considers the power framework identical impedance Z_s , the converter yield swell channel impedance Z_f , and the heap impedance Z_L . The four-leg PWM converter topology is appeared in Fig. 2. This converter topology is like the ordinary three-stage converter with the fourth leg associated with the impartial transport of the framework. The fourth leg builds changing states from 8 (23) to 16 (24), enhancing control adaptability and yield voltage quality, and is reasonable for current uneven remuneration

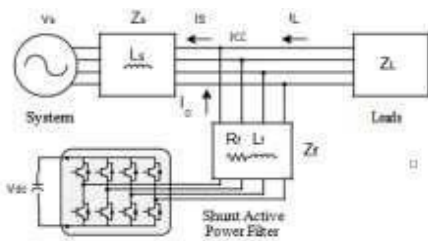


Fig 1. Three-phase equivalent circuit of the proposed shunt active power filter.

The voltage in any leg x of the converter, measured from the neutral point (n), can be expressed in terms of switching states, as follows:

$$v_{xN} = S_x v_{dc}, \quad x = u, v, w, n. \quad (1)$$

The mathematical model of the filter derived from the equivalent circuit shown in Fig. 2 is

$$v_o = v_{xN} - R_{eq} i_o - L_{eq} \frac{di_o}{dt}, \quad (2)$$

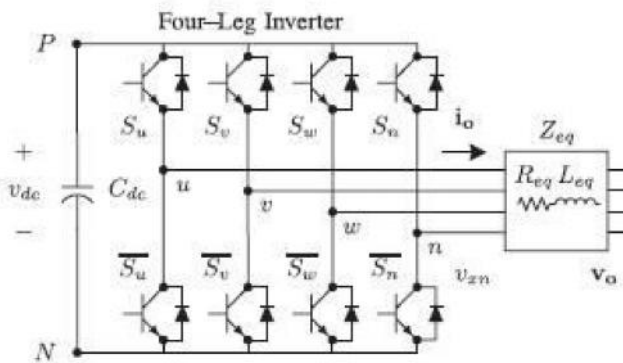


Fig. 2. Two-level four-leg PWM-VSI topology

where R_{eq} and L_{eq} are the 4L-VSI output parameters expressed as Thevenin impedances at the converter output terminals Z_{eq} .

Therefore, the Thevenin equivalent impedance is determined by a series connection of the ripple filter impedance Z_f and a parallel arrangement between the system equivalent impedance Z_s and the load impedance Z_L

$$Z_{eq} = \frac{Z_s Z_L}{Z_s + Z_L} + Z_f \approx Z_s + Z_f \quad (3)$$

For this model, it is assumed that $Z_L \gg Z_s$, that the resistive part of the system's equivalent impedance is neglected, and that the series reactance is in the range of 3–7% p.u., which is an acceptable approximation of the real system. Finally, in (2) $R_{eq} = R_f$ and $L_{eq} = L_s + L_f$.

I. DIGITAL PREDICTIVE CURRENT CONTROL.

The square graph of the proposed computerized prescient current control plot is appeared in Fig. 3. This control plot is essentially an improvement calculation and, along these lines, it must be actualized in a microchip. Therefore, the examination must be produced utilizing discrete science keeping in mind the end goal to consider extra limitations, for example, time postponements and approximations. The primary normal for prescient control is the utilization of the framework model to anticipate the future conduct of the factors to be controlled. The controller utilizes this data to choose the ideal exchanging state that will be connected to the power converter, as per predefined streamlining criteria. The prescient control calculation is anything but difficult to actualize and to comprehend, and it can be executed with three fundamental squares, as appeared in Fig. 3.

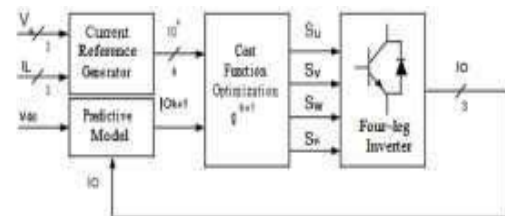


Fig. 3. Proposed predictive digital current control block diagram.

1) Current Reference Generator: This unit is intended to produce the required current reference that is utilized to remunerate the bothersome load current parts. For this situation, the system voltages, the heap streams, and the dc-voltage converter are estimated, while the unbiased yield present and nonpartisan load current are produced specifically from these signs (IV).

2) Prediction Model: The converter show is utilized to anticipate the yield converter current. Since the controller works in discrete time, both the controller and the framework demonstrate must be spoken to in a discrete time space [22]. The discrete time model comprises of a recursive grid condition that speaks to this expectation framework. This implies for a given inspecting time T_s , knowing the converter exchanging states and control factors at instant kT_s , it is conceivable to anticipate the following states at any instant $[k + 1]T_s$. Due to the first-order nature of the

state equations that describe the model in (1)–(2), a sufficiently accurate first-order approximation of the derivative is considered in this paper

$$\frac{dx}{dt} \approx \frac{x[k+1] - x[k]}{T_s} \quad (4)$$

The 16 possible output current predicted values can be obtained from (2) and (4) as

$$i_o[k+1] = \frac{T_s}{L_{eq}} (v_{rn}[k] - v_o[k]) + \left(1 - \frac{R_{eq} T_s}{L_{eq}}\right) i_o[k]$$

(5) As shown in (5), in order to predict the output current i_o at the instant $(k + 1)$, the input voltage value v_o and the converter output voltage v_{xN} , are required. The algorithm calculates all 16 values associated with the possible combinations that the state variables can achieve.

1) Cost Function Optimization: In order to select the optimal switching state that must be applied to the power converter, the 16 predicted values obtained for $i_o[k + 1]$ are compared with the reference using a cost function g , as follows:

$$g[k+1] = (i_{ou}^*[k+1] - i_{ou}[k+1])^2 + (i_{ov}^*[k+1] - i_{ov}[k+1])^2 + (i_{ow}^*[k+1] - i_{ow}[k+1])^2 + (i_{on}^*[k+1] - i_{on}[k+1])^2 \quad (6)$$

The yield current (i_o) is equivalent to the reference (i_o^*) when $g = 0$. Subsequently, the streamlining objective of the cost work is to accomplish a g esteem near zero. The voltage vector v_{xN} that limits the cost work is picked and after that connected at the next testing state. Amid each examining state, the exchanging express that produces the base estimation of g is chosen from the 16 conceivable capacity esteems. The calculation chooses the exchanging state that delivers this insignificant esteem and applies it to the converter amid the $k + 1$ state.

4) CURRENT REFERENCE GENERATOR

A dq-based current reference generator conspire is utilized to get the dynamic power channel current reference signals. This plan displays a quick and precise flag following capacity. This trademark dodges voltage variances that break down the present reference flag influencing remuneration execution [28]. The present reference signals are gotten from the relating load streams as appeared in Fig. 5. This module computes the reference flag streams required by the converter to repay receptive power, current symphonious, and current lopsidedness. The uprooting power factor ($\sin(L)$) and the greatest aggregate consonant twisting of

the heap (THD(L)) characterizes the connections between the evident power required by the dynamic power channel, as for the heap, as appeared where the value of THD(L) includes the maximum compensable harmonic current, defined as double the sampling frequency f_s . The frequency of the maximum current harmonic component that can be compensated is equal to one half of the converter switching frequency.

The dq-based scheme operates in a rotating reference frame; therefore, the measured currents must be multiplied by the $\sin(\omega t)$ and $\cos(\omega t)$ signals. By using dq-transformation, the d current component is synchronized with the corresponding phase-to-neutral system voltage, and the q current component is phase-shifted by 90° . The $\sin(\omega t)$ and $\cos(\omega t)$ synchronized reference signals are obtained from a synchronous reference frame (SRF) PLL. The SRF-PLL generates a pure sinusoidal waveform even when the system voltage is severely distorted. Tracking errors are eliminated, since SRF-PLLs are designed to avoid phase voltage unbalancing, harmonics (i.e., less than 5% and 3% in fifth and seventh, respectively), and offset caused by the nonlinear load conditions and measurement errors. Equation (8) shows the relationship between the real currents $i_{Lx}(t)$ ($x = u,$

v, w) and the associated dq components (i_d and i_q)

$$\begin{bmatrix} i_d \\ i_q \end{bmatrix} = \sqrt{\frac{2}{3}} \begin{bmatrix} \sin \omega t & \cos \omega t \\ -\cos \omega t & \sin \omega t \end{bmatrix} \begin{bmatrix} 1 & -\frac{1}{2} & -\frac{1}{2} \\ 0 & \frac{\sqrt{3}}{2} & -\frac{\sqrt{3}}{2} \end{bmatrix} \begin{bmatrix} i_{Lu} \\ i_{Lv} \\ i_{Lw} \end{bmatrix} \quad (8)$$

A low-pass filter (LFP) extracts the dc component of the phase currents i_d to generate the harmonic reference components i_d^* . The reactive reference components of the phase-currents are obtained by phase-shifting the corresponding ac and dc components of i_q by 180° . In order to keep the dc-voltage constant, the amplitude of the converter reference current must be modified by adding an active power reference signal i_e with the d -component, as will be explained in Section IV-A. The resulting signals i_d and i_q are transformed back to a three-phase system by applying the inverse Park and Clark transformation, as shown in (9). The cutoff frequency of the LFP used in this paper is 20 Hz.

(9)

$$\begin{bmatrix} i_{ou}^* \\ i_{ov}^* \\ i_{ow}^* \end{bmatrix} = \sqrt{\frac{2}{3}} \begin{bmatrix} \frac{1}{\sqrt{2}} & 1 & 0 \\ \frac{1}{\sqrt{2}} & -\frac{1}{2} & \frac{\sqrt{3}}{2} \\ \frac{1}{\sqrt{2}} & -\frac{1}{2} & -\frac{\sqrt{3}}{2} \end{bmatrix} \times \begin{bmatrix} 1 & 0 & 0 \\ 0 & \sin \omega t & -\cos \omega t \\ 0 & \cos \omega t & \sin \omega t \end{bmatrix} \begin{bmatrix} i_0 \\ i_d^* \\ i_q^* \end{bmatrix}$$

The current that flows through the neutral of the load is compensated by injecting the same instantaneous value obtained from the phase-currents, phase-shifted by 180°, as shown next

$$i_{on}^* = -(i_{Lu} + i_{Lv} + i_{Lw})$$

(10)

One of the real points of interest of the dq-based current reference generator is that it permits the usage of a direct controller in the dc-voltage control circle. Be that as it may, one critical inconvenience of the dq-based current reference calculation used to produce the present reference is that a second-order symphonic part is created in i_d and i_q under uneven working conditions. The adequacy of this consonant relies upon the percent of unequal load current (communicated as the connection between the negative grouping current $i_{L,2}$ and the positive arrangement current $i_{L,1}$). The second-order consonant can't be expelled from i_d and i_q , and in this manner produces a third symphonic in the reference current when it is changed over back to abc outline. Fig. 3 demonstrates the percent of framework current irregularity and the percent of third symphonic framework current, in capacity of the percent of load current unevenness. Since the heap current does not have a third symphonic, the one created by the dynamic power channel streams to the power framework. Fig. 4. dq-based Current Reference Generator Block Diagram.

II. Fuzzy controller

As of late, the number and assortment of uses of fluffly rationale have expanded altogether. The applications extend from buyer items, for example, cameras, camcorders, clothes washers, and microwaves to mechanical process control, medicinal instrumentation,

choice emotionally supportive networks, and portfolio choice.

To comprehend why utilization of fluffly rationale has developed, you should first comprehend what is implied by fluffly rationale. Fluffly rationale has two distinct implications. In a tight sense, fluffly rationale is a legitimate framework, which is an expansion of multivalve rationale. In any case, in a more extensive sense fluffly rationale (FL) is relatively synonymous with the hypothesis of fluffly sets, a hypothesis which identifies with classes of articles with unsharp limits in which participation involves degree. In this point of view, fluffly rationale in its limited sense is a branch of fl. Indeed, even in its more thin definition, fluffly rationale varies both in idea and substance from customary multivalve legitimate frameworks.

In fluffly Logic Toolbox programming, fluffly rationale ought to be deciphered as FL, that is, fluffly rationale in its wide sense. The fundamental thoughts hidden FL are clarified unmistakably and cleverly in Foundations of Fuzzy Logic. What may be included is that the essential idea hidden FL is that of a semantic variable, that is, a variable whose qualities are words instead of numbers. As a result, quite a bit of FL might be seen as a procedure for figuring with words as opposed to numbers. In spite of the fact that words are intrinsically less exact than numbers, their utilization is nearer to human instinct. Moreover, registering with words misuses the resistance for imprecision and accordingly brings down the cost of arrangement.

Another fundamental idea in FL, which assumes a focal part in the vast majority of its applications, is that of a fluffly if-then run or, essentially, fluffly run the show. In spite of the fact that lead based frameworks have a long history of utilization in Artificial Intelligence (AI), what is absent in such frameworks is a component for managing fluffly consequents and fluffly precursors. In fluffly rationale, this system is given by the analytics of fluffly guidelines. The math of fluffly tenets fills in as a reason for what may be known as the Fuzzy Dependency and Command Language (FDCL).

III. SIMULATION RESULTS

A reproduction demonstrate for the three-stage four-leg PWM converter with the parameters appeared in Table I has been produced utilizing MATLAB-Simulink. The objective is to verify the current harmonic remuneration adequacy of the proposed control plot under various working conditions. A six-beat rectifier was utilized as a nonlinear load. The proposed predictive control algorithm was customized utilizing a S-work obstruct that permits reenactment of a discrete model that can be effortlessly actualized in a continuous

interface (RTI) on the dSPACE DS1103 R&D control board. Reproductions were performed considering a 20 [μs] of test time. In the reenacted comes about appeared in Fig. 8, the dynamic channel begins to remunerate at $t = t_1$. Right now, the dynamic power channel infuses a yield current i_{ou} to repay current consonant segments, current lopsided, and nonpartisan current at the same time. Amid remuneration, the framework streams is demonstrate sinusoidal waveform, with low aggregate symphonious contortion (THD = 3.93%). At $t = t_2$, a three-stage adjusted load step change is produced from 0.6 to 1.0 p.u. The remunerated framework streams stay sinusoidal regardless of the adjustment in the heap current extent. At last, at $t = t_3$, a solitary stage stack step change is presented in stage u from 1.0 to 1.3 p.u., which is equal to a 11% current unevenness. Of course on the heap side, an impartial current moves through the unbiased conductor (i_{Ln}), yet on the source side, no nonpartisan current is watched (i_{sn}). Reproduced comes about demonstrate that the proposed control plot adequately dispenses with lopsided streams.

Also, Fig. 4 demonstrates that the dc-voltage stays stable all through the entire dynamic power channel activity.

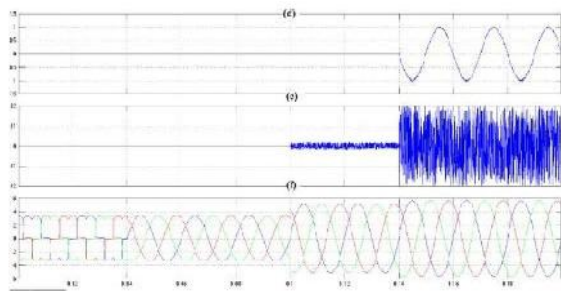


Fig. 4 . Simulated waveforms of the proposed control scheme.

- (a) Phase to neutral source voltage.
- (b) Load Current.
- (c) Active power filter output current.
- (d) Load neutral current.
- (e) System neutral current.
- (f) System currents.
- (g) DC voltage converter

II. CONCLUSION

Improved dynamic current harmonics and a reactive power compensation scheme for power distribution systems with generation from renewable sources has been proposed to improve the current quality of the distribution system. Advantages of the proposed scheme are related to its simplicity, modeling, and implementation.

REFERENCES

- [1] Pablo Acuña, Member, IEEE, Luis Morán, Fellow, IEEE, Marco Rivera, Member, IEEE, Juan Dixon, Senior Member, IEEE, and José Rodríguez, Fellow, IEEE, "Improved Active Power Filter Performance for Renewable Power Generation Systems" *IEEE TRANSACTIONS ON POWER ELECTRONICS*, VOL. 29, NO. 2, FEBRUARY 2014 687
- [2] J. Rocabert, A. Luna, F. Blaabjerg, and P. Rodríguez, "Control of power converters in AC microgrids," *IEEE Trans. Power Electron.*, vol. 27, no. 11, pp. 4734–4749, Nov. 2012.
- [3] M. Aredes, J. Hafner, and K. Heumann, "Three-phase four-wire shunt active filter control strategies," *IEEE Trans. Power Electron.*, vol. 12, no. 2, pp. 311–318, Mar. 1997.
- [4] S. Naidu and D. Fernandes, "Dynamic voltage restorer based on a fourleg voltage source converter," *Gener. Transm. Distrib., IET*, vol. 3, no. 5, pp. 437–447, May 2009.
- [5] N. Prabhakar and M. Mishra, "Dynamic hysteresis current control to minimize switching for three-phase four-leg VSI topology to compensate nonlinear load," *IEEE Trans. Power Electron.*, vol. 25, no. 8, pp. 1935–1942, Aug. 2010.
- [6] V. Khadkikar, A. Chandra, and B. Singh, "Digital signal processor implementation and performance evaluation of split capacitor, four-leg and three h-bridge-based three-phase four-wire shunt active filters," *Power Electron., IET*, vol. 4, no. 4, pp. 463–470, Apr. 2011.
- [7] F. Wang, J. Duarte, and M. Hendrix, "Grid-interfacing converter systems with enhanced voltage quality for microgrid application; concept and implementation," *IEEE Trans. Power Electron.*, vol. 26, no. 12, pp. 3501–3513, Dec. 2011.
- [8] X. Wei, "Study on digital pi control of current loop in active power filter," in *Proc. 2010 Int. Conf. Electr. Control Eng.*, Jun. 2010, pp. 4287–4290.
- [9] R. de Araujo Ribeiro, C. de Azevedo, and R. de Sousa, "A robust adaptive control strategy of active power filters for power-factor correction, harmonic compensation, and balancing of nonlinear loads," *IEEE Trans. Power Electron.*, vol. 27, no. 2, pp. 718–730, Feb. 2012.
- [10] J. Rodríguez, J. Pontt, C. Silva, P. Correa, P. Lezana, P. Cortes, and U. Ammann, "Predictive current control of a voltage source inverter," *IEEE Trans. Ind. Electron.*, vol. 54, no. 1, pp. 495–503, Feb. 2007.